**J NeuroOncol**

# Long-term exposure to irinotecan reduces cell migration in glioma cells

Al-Ghafari, A.B[1*]., Punjaruk, W[2*]., Storer, L[2]., Carrier, D.J.[2], Hussein, D[2]., Coyle, B[2#]., Kerr, I.D[1#].

[1] School of Life Sciences, Queen's Medical Centre, University of Nottingham, Nottingham, NG7 2UH

[2] School of Medicine, Queen's Medical Centre, University of Nottingham, Nottingham, NG7 2UH

* - these authors contributed equally to data generation.

# - authors to whom correspondence may be addressed.

Ian.kerr@nottingham.ac.uk tel: 00 44 8230122

Beth.coyle@nottingham.ac.uk tel: 00 44 8230719

Keywords: glioma; topoisomerase; etoposide; irinotecan; ABCB1; invasion; chemotherapy

## Introduction

Glioblastoma multiforme (GBM) is the most common malignant brain tumour in adults (annual incidence 3 per 100,000; [1]). It carries a very poor prognosis with mean overall survival of 12-17 months. Despite testing a multitude of chemotherapy agents and strategies, very little progress has been made in extending the life expectancy of those diagnosed with a GBM, since the establishment of the Stupp protocol (a combination of radiotherapy and temozolomide) a decade ago [2, 3]. This is believed to be due to a high level of intrinsic drug resistance [4] combined with the fact that these tumours tend to diffusely invade the local brain parenchyma making it difficult to identify the perimeter and effectively remove them surgically [5-7]. An improvement in clinical outcome therefore requires identification of drugs that can inhibit invasion as well as promote cell death.

Antineoplastic effects of topoisomerase inhibitors have been observed in glioma cells. Topoisomerases are enzymes involved in cleaving and religating supercoiled DNA. Topoisomerase I does this through making single strand breaks whereas topoisomerase II breaks both strands. Inhibition of either enzyme results in cell death and cancer cells have been shown to be selectively sensitive to topoisomerase inhibitors. Indeed there are a number of ongoing glioma clinical trials exploring the combination of established inhibitors with other marketed drugs e.g. the phase II clinical trial NCT01574092 is assessing irinotecan (topoisomerase I inhibitor) in combination with cisplatin. In addition to which, small molecule inhibitors such as the topoisomerase II inhibitor Banoxantrone (phase I/II) or the topoisomerase I inhibitors Cositecan (phase I) and Gimatecan (phase I) are also currently in clinical trials [8]. Over time, however, studies have shown that many tumours become resistant to topoisomerase II inhibitors due to increased DNA repair or acquired mutations in topoisomerase II [9, 10], although whether this is paralleled by an increase in general drug resistance mechanisms (e.g. multidrug efflux pumps) is unknown.

In this study, we set out to determine the cellular effects of long-term exposure to topoisomerase inhibitors in a glioma cell line (C6), focusing on acquired cross-resistance and invasion. The C6 glioma cell line was grown out from a glioma induced in an outbred Wistar rat strain by repeated rounds of treatment with N'N'-methylnitrosourea [11, 12]. Injection of the C6 cell line into newborn rats produced a tumour with pathology consistent with a glioblastoma multiforme including a diffuse invading border [13]. Since then it has been used as an experimental model in a number of different studies (reviewed in [14]). C6 cells were continuously exposed to either a topoisomerase I inhibitor (irinotecan) or a topoisomerase II inhibitor (etoposide). In common with other studies we found that continuous treatment with etoposide resulted in increased resistance to this agent, but

did not induce cross-resistance to irinotecan. In contrast, even after many rounds of exposure to the irinotecan, sensitivity to this drug was maintained and, importantly, we also observed a reduction in migratory capacity of treated cells. This data argues for the further clinical investigation of topoisomerase I inhibition as a mechanism to limit glioma invasion without incurring increased resistance to chemotherapy.

## Materials and Methods

### Cell culture

The rat C6 glioma cell line was maintained at 37˚C/5% $CO_2$ in Dulbecco's Modified Eagle Medium (DMEM) (Invitrogen) with 10% foetal bovine serum (FBS). Drug selected cell lines (C6-etoposide and C6-irinotecan) were established by continuous culture over 5 passages at the drug concentration established to cause death of 70% of cells i.e.in the presence of 16 µM etoposide (Sigma) and 10 µM irinotecan (Sigma). In the case of etoposide selection, cells were incubated for 2 hours [15] and then media was changed while for irinotecan selection, cells were incubated for 96 hours then media was changed [16]. Similarly, in experiments with prolonged duration such as clonogenic assays, the drugs were removed after 2 hours and 96 hours for etoposide and irinotecan, respectively.

### Western blot analysis

Cell pellets were resuspended in PBS/glycerol (10% v/v) supplemented with EDTA free protease inhibitor cocktail set III (Calbiochem) and lysed by probe sonication for 3 x 10-20 second bursts. Equal quantities of total protein were resolved on 8-12% w/v polyacrylamide gels and protein was transferred to Hybond™–P PVDF membrane (Amersham Biosciences). Membranes were blocked with 5% w/v non- fat Marvel milk in TBST buffer (25 mM Tris pH 7.6, 0.15 M NaCl, 0.1% v/v Tween-20) at room temperature for an hour followed by incubation with primary antibodies (dilutions given in figure legends) at 4°C overnight. The membranes were then washed with TBST and incubated for 1 hour at room temperature with horseradish peroxidase conjugated secondary antibodies. Following washing, the specific proteins were detected using a SuperSignal® West Pico Chemilluminescent Substrate (Thermo Scientific). Where band intensity was quantified, the density of unsaturated exposures was determined with Scion Image software (NIH, USA) after scanning the blots at 600 dpi resolution.

**Quantitative RT- PCR analysis**

RNA was isolated using a *mir*Vana™ miRNA isolation kit (Ambion) and transcribed into cDNA using Superscript III reverse transcriptase (Invitrogen). Quantitative reverse transcription PCR (qPCR) analysis was carried out using a CFX96 real-time PCR machine (Biorad) and iQ SYBR Green Superrmix (Biorad; primers in Supplementary Table 1). Samples were analysed in triplicate and data obtained from three independent experiments were used for analysis of relative gene expression compared to GAPDH and β-Actin [17] with the Pfaffl equation [18].

**Clonogenic assay**

Viability was determined following an established clonogenic assay protocol [19]. Approximately 100 cells were seeded in a 2 ml volume into a 6 well plate and were treated with etoposide (5 - 80 μM), irinotecan (0.5 - 24 μM) or a vehicle control (DMSO either 0.08% v/v or 0.02% v/v for etoposide and irinotecan respectively). Plates were incubated for 7-10 days until colonies containing approximately 50 cells were visible in control wells. Subsequently, media was removed and colonies were fixed with paraformaldehyde (4% (w/v) PFA in PBS, 20 minutes) and stained with crystal violet (0.1% (w/v) in distilled $H_2O$, 5 minutes), prior to colony counting.

**Flow cytometry**

Single cell suspensions (2 x $10^6$ cells/ 0.1 ml) in fluorescent activated cell sorting (FACS) buffer (0.5% w/v BSA in phenol red free DMEM) were incubated with rhodamine 123 (2 μM) and periodically inverted during a 30 minute incubation at 37°C. Cells were washed twice by pelleting (250g, 3 minutes, 4°C) and resuspension in FACS buffer. Cellular fluorescence was determined using a Cytomics FC500 (Beckman Coulter) flow cytometer and data analysed with WinMDI (Scripps Institute).

**Reactive oxygen species (ROS) assay**

Black clear-bottom 96-well plates (Greiner Bio-one) were seeded with 10,000 cells per well. After overnight incubation, media was replaced by Hanks Balanced Salt Solution (HBSS) supplemented with 50 μM 2',7'-dichlorofluorescin diacetate (DCFH-DA; Invitrogen) and the plate was incubated in a 37˚C/5% $CO_2$ incubator for 30 minutes. Excess DCFH-DA was removed by washing with HBSS. ROS

production was then induced by incubation with indicated concentrations of tert-butyl hydroperoxide (TBHP) (Sigma). The increase in DCF fluorescence (indicative of ROS production) was measured ($\lambda_{Ex}$ 485nm; $\lambda_{Em}$ 530nm) on a Flexstation 3 fluorescence microplate reader (Molecular Devices, USA) over a 3 hour period. Rates of ROS production were determined across the linear region of the time course (typically 60-90 minutes) and fold-changes in the rate of ROS production were determined compared to cells without TBHP treatment.

**Wound scratch assay**

Cells ($0.5x10^6$ in DMEM containing 10% FBS) were seeded in duplicate sterile 6-well plates and incubated overnight in 37˚C/5% $CO_2$. A scratch was then made across the centre of each well with a sterile 200 µl pipette tip. Cell migration was assessed with time lapse microscopy (LEICA DMIRB Microscope, LEICA Microsystem) at 37˚C for up to 65 hours. Images were taken with brightfield 10x phase contrast objective lens, every 30 minutes at three different positions along each scratch. All images were analysed using ImageJ software to determine the wound size relative to the initial scratch.

**Transwell migration assay**

A transwell migration assay was performed to determine the migration response under the influence of a chemo-attractant (10% FBS). Experiments were performed using the ChemoTx®System kit (Neuro Probe) according to the manufacturer's instructions. Cells ($2x10^4$) were added to the upper filter and migration towards the chemo-attractant (with HBSS as control) occurred during incubation for 24 hours (37˚C/5% $CO_2$). Following the incubation, the media was aspirated and cells were fixed (4% PFA in PBS, 20 minutes), prior to nuclear DNA staining with Hoechst 33342 for 5 minutes. Filters were washed once with PBS and the microplate was scanned on an ImageXpressMICRO (Molecular Devices, USA) to determine the total number of migrated cells.

**Statistical analysis**

All experiments were conducted on at least three independent occasions. GraphPad Prism (GraphPad Software, San Diego California USA) was used for all data fitting and statistical data analysis. Clonogenic assay data were fitted to the general sigmoidal dose response equation. Wound

closure data was fitted using exponential decay equations. ROS production rates were determined using linear regression. Where data from multiple experiments are displayed in column format the error bars represent the standard error of the mean. Statistical significance was analysed by one way ANOVA or unpaired t-test (as described in figure legends) to compare between cell lines. A *P* value smaller than 0.05 ($P<0.05$) was considered significant.

**Results:**

Understanding of glioma drug resistance and local invasion is critical if we are to develop better therapies for this type of brain tumour. We were interested in observing whether changes in drug resistance and invasion occurred, in a model glioma cell line (C6), following exposure to topoisomerase I and topoisomerase II inhibition. Initially, we explored whether etoposide (topoisomerase II inhibitor) and irinotecan (topoisomerase I inhibitor) were cytotoxic against the C6 cell line and used a clonogenic assay to determine $IC_{50,70}$ values (the concentration of drug required to achieve 50 or 70%-maximal inhibition of colony growth; Figure 1). The colony formation of the C6 cell line following a single exposure to either drug could be inhibited by low micromolar concentrations of both drugs ($IC_{50}$ for etoposide 8.6 ± 0.6 μM; $IC_{50}$ for irinotecan 5.3 ± 0.4 μM). Since chemotherapy is normally given to patients in cycles, consisting of a weekly dose for several weeks then a period of rest followed by further cycles, we investigated how C6 cells would respond to chronic cyclical exposure to topoisomerase inhibitors at cytotoxic concentrations. Therefore, we cultured cells for multiple passages in the presence of $IC_{70}$ concentrations of etoposide or irinotecan (16 μM and 8 μM respectively), resulting in the production of sub-lines called C6-Et (for a cell line cultured in the presence of etoposide) and C6-Ir (for a cell line cultured in the presence of irinotecan. A further cell line (C6-V) was established after continuous culture in the presence of DMSO (0.05% v/v*)*, the solvent for both drugs.

A common mechanism that might be expected to show alteration upon drug selection is the up-regulation of ABC transporters of the multidrug resistance family [20]. We saw increased expression of ABCB1/P-glycoprotein in both cell lines compared to a DMSO (vehicle control) selected C6 cell line (Figure 2A). Similarly, a functional assay, based upon extrusion of the fluorescent dye rhodamine 123 (R123) by ABCB1-expressing cells, demonstrated that the percentage of cells capable of exporting R123 increased to over 75% in both selected cell lines (Figure 2B). For comparison, the DMSO-treated C6 cell line showed R123 extrusion in 35% of cells, a value identical to that of the parental C6

cell line (Figure 2B). Thus, both cell lines displayed elevated ABCB1 expression and function following continuous exposure to topoisomerase inhibitors. In contrast, ABCG2 (breast cancer resistance protein) was not detected either before or after drug selection of the C6 cell line, and ABCC1 (multidrug resistance associated protein 1) was only expressed after exposure of cell lines to topoisomerase inhibitors for greater than 10 passages, culture conditions that were not typical in our experiments (data not shown).

We then examined whether the increase in ABCB1 expression was associated with increased resistance to the topoisomerase inhibitor used in their selection, or with acquired cross-resistance. In clonogenic assays, the C6-Et cell line showed an increase (2.5-fold; $p < 0.05$; Figure 3A) in the $IC_{70}$ for etoposide but showed no cross-resistance to irinotecan, although both drugs are ABCB1 substrates [21]. The modest increase in resistance to etoposide upon continuous exposure without associated cross-resistance leads us to propose that the mechanism of elevated resistance is not solely via a classical multidrug export pump, and that other mechanism(s) of drug resistance, or protection against the damaging effects of etoposide is more active in the C6-Et cell line. Conversely, the C6-Ir cell line maintained the same $IC_{70}$ for irinotecan compared to the C6-V cell line (Figure 3B), i.e. growing C6 cells in the presence of irinotecan did not result in the selection of cells with elevated irinotecan resistance, in agreement with studies indicating that ABCB1, although capable of transporting irinotecan [21], is not able to establish substantial concentration gradients of this drug [22].

Resistance to chemotherapy in cancer cell lines has also been associated with the emergence of a sub-population of cells that displays lower levels of reactive oxygen species, and concomitant elevation of antioxidant enzyme expression [23]. We investigated whether this was true for the drug exposed C6 cell lines by determining their ROS production rates following incubation with tertiary butyl hydroperoxide. ROS production rates were linear for at least 60 minutes following TBHP administration, and were consistent in all three cell lines at multiple concentrations of TBHP (Figure 4A; ANOVA $P > 0.05$), indicating that the cell lines do not differ in their ability to respond to ROS production. In confirmation of this, the expression level of ROS-detoxifying enzymes (e.g. catalase) was equal across the 3 cell lines (Figure 4B, C). This suggests that the prolonged exposure to irinotecan or etoposide does not result in the emergence of a cell population better able to respond to oxidative stress.

One of the hallmarks of glioma is local invasion [5, 7] , and it was therefore of interest to determine cell migration following drug exposure in a glioma cell line model. Monolayers of C6-V, C6-Et and C6-Ir cells were scratch-wounded with a sterile 0.2ml pipette tip and the rate of migration into the cell free area monitored by time-lapse microscopy. Apparent from the still images taken from time-lapse videos is the reduced wound closure in irinotecan treated cells (Figure 5A, compare for example the 16 and 24 hour time points). The size of the wound was measured at 30 minute intervals allowing for a single exponential fit of the data (Figure 5B) to determine the half-time for wound closure. Two of the three cell lines fitted a single exponential equation, whilst the fitting of the C6-Et cell line data required the presence of a short lag phase before an exponential decay. Non-linear regression of the data shows that the C6-Ir cell line closed the wound significantly slower ($t_{1/2}$ = 720 ± 35 mins) than the other two cell lines (C6-Et $t_{1/2}$ 457 ± 24 mins, parental C6 cell line $t_{1/2}$ 294 ± 24 mins). A similar reduction in migratory ability for the C6-Ir cell line was observed with transwell migration assays (Figure 5C).A potential molecular basis of this reduced rate of migration was investigated by determining the expression of collagens Col1A2 and Col3A1, both of which are implicated in tumour invasion and/or epithelia to mesenchymal transition [24]. For Col3A1, the C6-Ir cell line showed a significantly reduced gene expression compared to the C6-Et and C6-V cell line (Figure 5D), and for Col1A2 C6-Ir also showed reduced gene expression compared to the C6-Et (Figure 5E).

**Discussion**

In this study we compared the effect of two established antineoplastic agents (the topoisomerase II inhibitor etoposide and the topoisomerase I inhibitor irinotecan) on glioma cell line drug resistance and invasion. Instead of monitoring glioma cell response to a single exposure, we focused instead on cellular response after several rounds of treatment (mirroring the clinical regimen). What we observed was that C6 glioma cells do not acquire additional resistance to irinotecan when continuously treated with this type I topoisomerase I inhibitor. In contrast, C6 cells became more resistant to etoposide after several rounds of treatment with this type II topoisomerase inhibitor. Analysis of C6-Et cells revealed that they had increased expression of the multidrug transporter ABCB1. An increase in ABCB1 expression was however observed in cells treated with both etoposide and irinotecan, but only resistance to etoposide was increased, and this was in the absence of cross-resistance to irinotecan. Hence, although ABCB1 is upregulated this does not appear to be a major drug resistance mechanism in these cells. We also assayed the ability of our continuously exposed

cells to withstand reactive oxygen species, but saw no change in this ability. The resistance to etoposide therefore appears to be highly specific and the majority of resistance is probably due to a mutation within topoisomerase II itself preventing interaction with etoposide [9] or an increase in the rate of DNA repair [10]. These data indicate that etoposide is a poor choice for cyclical therapy in glioma as it leads to elevated etoposide resistance. Continuous exposure to irinotecan, on the other hand, does not lead to increased resistance to itself or cross-resistance to etoposide.

Local invasion is a major problem in glioma and makes it difficult to completely surgically remove these tumours. Glioma cells have been shown to be able to produce their own extracellular matrix factors including collagens [25] and high concentrations of collagen in the glioma microenvironment have been shown to correlate with more effective migration [24]. C6 glioma cells produce a diffusely invading tumour in animal models and so may be more useful for modelling invasion *in vitro* compared to U87 cells which produce more circumscribed tumours. We observed a reduced migratory capacity of C6 cells treated with repeated cycles of irinotecan, and a reduction in expression of collagen Col3A1 suggestive that impaired migration may be due to inhibition of cell matrix interactions that are essential for tumour invasion. In contrast, etoposide treated cells which show rapid wound closure also display elevated collagen expression, suggesting that treatment has selected cells with an increased migratory capacity which would be an undesirable effect in therapy. Although there are no clinical reports of increased metastatic potential of etoposide treated tumours, there are growing reports that tumour drug resistance and invasion are interlinked and our data further contributes to this emerging picture [26-29].

In conclusion, repeated rounds of treatment of glioma cells with the topoisomerase I inhibitor irinotecan does not result in increased drug resistance or ROS resistance, rather it produces a cell line with impaired migration, supporting further the investigation of irinotecan and derivatives in treatment of glioma.

**Acknowledgements**

We deeply appreciate support from the Royal Thai government for a PhD scholarship for WP, and King Abdulaziz University for a PhD scholarship for ABA. This work was supported by funding from

the Brain Tumour Charity (SDBTT 17/3). The authors are grateful to Dr Peter Jones (Life Sciences, University of Nottingham) for the generous donation of transwell migration plates.

**References**

1. Dolecek TA, Propp JM, Stroup NE, Kruchko C (2012) CBTRUS statistical report: primary brain and central nervous system tumors diagnosed in the United States in 2005-2009. Neuro-oncology 14 Suppl 5: v1-49 doi:10.1093/neuonc/nos218
2. Stupp R, Mason WP, van den Bent MJ, Weller M, Fisher B, Taphoorn MJ, Belanger K, Brandes AA, Marosi C, Bogdahn U, Curschmann J, Janzer RC, Ludwin SK, Gorlia T, Allgeier A, Lacombe D, Cairncross JG, Eisenhauer E, Mirimanoff RO (2005) Radiotherapy plus concomitant and adjuvant temozolomide for glioblastoma. The New England journal of medicine 352: 987-996 doi:10.1056/NEJMoa043330
3. Gilbert MR, Wang M, Aldape KD, Stupp R, Hegi ME, Jaeckle KA, Armstrong TS, Wefel JS, Won M, Blumenthal DT, Mahajan A, Schultz CJ, Erridge S, Baumert B, Hopkins KI, Tzuk-Shina T, Brown PD, Chakravarti A, Curran WJ, Jr., Mehta MP (2013) Dose-dense temozolomide for newly diagnosed glioblastoma: a randomized phase III clinical trial. Journal of clinical oncology : official journal of the American Society of Clinical Oncology 31: 4085-4091 doi:10.1200/JCO.2013.49.6968
4. Haar CP, Hebbar P, Wallace GCt, Das A, Vandergrift WA, 3rd, Smith JA, Giglio P, Patel SJ, Ray SK, Banik NL (2012) Drug resistance in glioblastoma: a mini review. Neurochemical research 37: 1192-1200 doi:10.1007/s11064-011-0701-1
5. Cuddapah VA, Robel S, Watkins S, Sontheimer H (2014) A neurocentric perspective on glioma invasion. Nature reviews Neuroscience 15: 455-465 doi:10.1038/nrn3765
6. Paw I, Carpenter RC, Watabe K, Debinski W, Lo HW (2015) Mechanisms regulating glioma invasion. Cancer letters 362: 1-7 doi:10.1016/j.canlet.2015.03.015
7. Sanai N, Berger MS (2008) Glioma extent of resection and its impact on patient outcome. Neurosurgery 62: 753-764; discussion 264-756 doi:10.1227/01.neu.0000318159.21731.cf
8. Prabhu S, Harris F, Lea R, Snape TJ (2014) Small-molecule clinical trial candidates for the treatment of glioma. Drug discovery today 19: 1298-1308 doi:10.1016/j.drudis.2014.02.007
9. Chikamori K, Grabowski DR, Kinter M, Willard BB, Yadav S, Aebersold RH, Bukowski RM, Hickson ID, Andersen AH, Ganapathi R, Ganapathi MK (2003) Phosphorylation of serine 1106 in the catalytic domain of topoisomerase II alpha regulates enzymatic activity and drug sensitivity. The Journal of biological chemistry 278: 12696-12702 doi:10.1074/jbc.M300837200
10. Adachi N, Suzuki H, Iiizumi S, Koyama H (2003) Hypersensitivity of nonhomologous DNA end-joining mutants to VP-16 and ICRF-193: implications for the repair of topoisomerase II-mediated DNA damage. The Journal of biological chemistry 278: 35897-35902 doi:10.1074/jbc.M306500200
11. Benda P, Lightbody J, Sato G, Levine L, Sweet W (1968) Differentiated rat glial cell strain in tissue culture. Science 161: 370-371
12. Schmidek HH, Nielsen SL, Schiller AL, Messer J (1971) Morphological studies of rat brain tumors induced by N-nitrosomethylurea. Journal of neurosurgery 34: 335-340 doi:10.3171/jns.1971.34.3.0335
13. Auer RN, Del Maestro RF, Anderson R (1981) A simple and reproducible experimental in vivo glioma model. The Canadian journal of neurological sciences Le journal canadien des sciences neurologiques 8: 325-331
14. Barth RF, Kaur B (2009) Rat brain tumor models in experimental neuro-oncology: the C6, 9L, T9, RG2, F98, BT4C, RT-2 and CNS-1 gliomas. Journal of neuro-oncology 94: 299-312 doi:10.1007/s11060-009-9875-7
15. Hande KR (1998) Etoposide: four decades of development of a topoisomerase II inhibitor. Eur J Cancer 34: 1514-1521

16. Pollack IF, Erff M, Bom D, Burke TG, Strode JT, Curran DP (1999) Potent topoisomerase I inhibition by novel silatecans eliminates glioma proliferation in vitro and in vivo. Cancer research 59: 4898-4905
17. Vandesompele J, De Preter K, Pattyn F, Poppe B, Van Roy N, De Paepe A, Speleman F (2002) Accurate normalization of real-time quantitative RT-PCR data by geometric averaging of multiple internal control genes. Genome biology 3: RESEARCH0034
18. Pfaffl MW (2001) A new mathematical model for relative quantification in real-time RT-PCR. Nucleic acids research 29: e45
19. Franken NA, Rodermond HM, Stap J, Haveman J, van Bree C (2006) Clonogenic assay of cells in vitro. Nature protocols 1: 2315-2319 doi:10.1038/nprot.2006.339
20. Kartner N, Riordan JR, Ling V (1983) Cell surface P-glycoprotein associated with multidrug resistance in mammalian cell lines. Science 221: 1285-1288
21. Szakacs G, Paterson JK, Ludwig JA, Booth-Genthe C, Gottesman MM (2006) Targeting multidrug resistance in cancer. Nature reviews 5: 219-234
22. Goldwirt L, Beccaria K, Carpentier A, Farinotti R, Fernandez C (2014) Irinotecan and temozolomide brain distribution: a focus on ABCB1. Cancer chemotherapy and pharmacology 74: 185-193 doi:10.1007/s00280-014-2490-0
23. Achuthan S, Santhoshkumar TR, Prabhakar J, Nair SA, Pillai MR (2011) Drug-induced senescence generates chemoresistant stemlike cells with low reactive oxygen species. The Journal of biological chemistry 286: 37813-37829 doi:10.1074/jbc.M110.200675
24. Kaufman LJ, Brangwynne CP, Kasza KE, Filippidi E, Gordon VD, Deisboeck TS, Weitz DA (2005) Glioma expansion in collagen I matrices: analyzing collagen concentration-dependent growth and motility patterns. Biophysical journal 89: 635-650 doi:10.1529/biophysj.105.061994
25. Paulus W, Huettner C, Tonn JC (1994) Collagens, integrins and the mesenchymal drift in glioblastomas: a comparison of biopsy specimens, spheroid and early monolayer cultures. International journal of cancer Journal international du cancer 58: 841-846
26. Coyle B, Kessler M, Sabnis DH, Kerr ID (2015) ABCB1 in children's brain tumours. Biochemical Society transactions 43: 1018-1022 doi:10.1042/BST20150137
27. Othman RT, Kimishi I, Bradshaw TD, Storer LC, Korshunov A, Pfister SM, Grundy RG, Kerr ID, Coyle B (2014) Overcoming multiple drug resistance mechanisms in medulloblastoma. Acta neuropathologica communications 2: 57 doi:10.1186/2051-5960-2-57
28. Colone M, Calcabrini A, Toccacieli L, Bozzuto G, Stringaro A, Gentile M, Cianfriglia M, Ciervo A, Caraglia M, Budillon A, Meo G, Arancia G, Molinari A (2008) The multidrug transporter P-glycoprotein: a mediator of melanoma invasion? The Journal of investigative dermatology 128: 957-971 doi:10.1038/sj.jid.5701082
29. Miletti-Gonzalez KE, Chen S, Muthukumaran N, Saglimbeni GN, Wu X, Yang J, Apolito K, Shih WJ, Hait WN, Rodriguez-Rodriguez L (2005) The CD44 receptor interacts with P-glycoprotein to promote cell migration and invasion in cancer. Cancer research 65: 6660-6667 doi:10.1158/0008-5472.CAN-04-3478

**Figure Legends**

**Figure 1. The glioma cell line C6 is sensitive to DNA topoisomerase inhibitors. A**, **B** clonogenic assays of C6 cells were performed in the presence of increasing concentrations of etoposide (**A**) or irinotecan (**B**) resulting in dose-dependent inhibition of colony growth. The mean $IC_{70}$ concentrations are 16.2 μM for etoposide and 7.6 μM for irinotecan. All data are derived from at least 3 independent experiments and error bars denote the standard error of the mean.

**Figure 2. Expression and function of ABCB1 is increased in drug exposed C6 sub-lines**. **A.** Microsomal membrane fractions (40 μg) of the indicated C6 cell lines were resolved on 8% w/v polyacrylamide gels and, following electro-transfer, membranes were probed with anti-ABCB1 antibody C219 (1:1000). Blots were subsequently re-probed with anti-tubulin antibodies. Results are representative of at least 3 independent experiments. ABCB1 is observed as a two bands indicative of glycosylation. **B**. ABCB1 function was confirmed in a flow cytometry assay in which the percentage of cells exporting rhdoamine-123 (R123) was determined. Results are the mean (s.e.m.) of at least 3 independent experiments. Data were compared using ANOVA and Newman-Kuels post-test. Cell lines showing increased % of rhodamine extruding cells compared to vector treated controls are designated by * ($p < 0.05$) and ** ($p < 0.01$).

**Figure 3. Continuous exposure of C6 to etoposide, but not to irinotecan, results in selection of a more drug resistant population.** The resistance of parental C6 and drug exposed sub-lines lines was assessed by clonogenic assays (**A, B**). The C6-Et line showed increased resistance to etoposide compared to the other cell lines (**A,** $p < 0.05$; ANOVA), whereas the C6-Ir cell line showed no increase in resistance (**B)**. The C6-Et cell line did not exhibit cross-resistance to irinotecan.

**Figure 4. Prolonged exposure to DNA topoisomerase inhibitors is not associated with increased resistance to ROS. A** Cells were cultured in the absence or presence of a reactive oxygen species inducer (TBHP) and a fluorescent indicator of ROS production (DCF). A linear rate of ROS production was measured over 60 minutes following TBHP addition (relative fluorescence units/minute). Relative rates of ROS production compared to untreated cells were calculated over this linear period and displayed as a function of TBHP concentration. **B, C.** Expression of catalase was determined by western blotting using polyclonal anti catalase antibody at 1:500 dilution (Abcam) and relative

expression determined by comparison to actin band intensity (AC-74 monoclonal antibody at 1:5000 dilution) (**C**). All data represents the mean (s.e.m.) of at least 3 independent experiments.

**Figure 5. Exposure to irinotecan results in reduced migration and expression of collagens. A** Wound scratch healing assays were analysed by time-lapse microscopy, and representative images in the time-lapse are shown. **B** Wound closure is represented in the form of percentage initial scratch size as a function of time. Individual data points and errors are omitted for clarity (as each line results from >130 data points). Non-linear regression of the data shows that the C6-Ir cell line closed the wound significantly slower ($t_{1/2}$ = 720 ± 35 mins) than the C6-Et (457 ± 24 mins) and parental C6 cell line. **C**. Transwell migration assays demonstrate that C6-Ir displays a reduced migration in response to a chemoattractant compared to C6-Et. **D, E** qPCR of collagens 3A1 (**D**) and 1A2 (**E**) demonstrates reduced collagen expression in the C6-irinotecan cell line compared to the C6-etoposide cell line (p-vales obtained from post-test comparisons following ANOVA, * $p < 0.05$, ** $P < 0.01$, *** $P < 0.001$). The relative expression of the collagens was determined compared to the geometric mean of two "housekeeping genes" GAPDH and B-actin. All data represents the mean (s.e.m.) of at least 3 independent experiments.

Figure 1

A

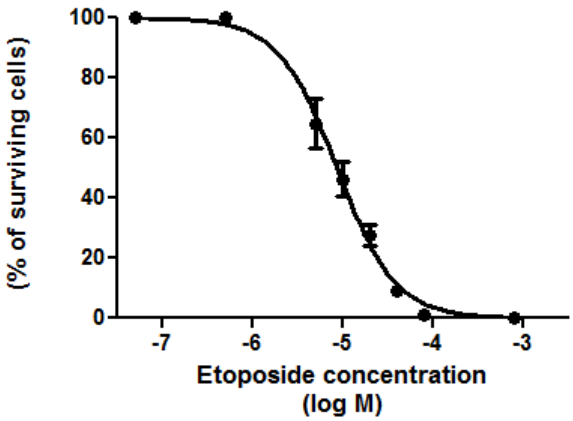


B

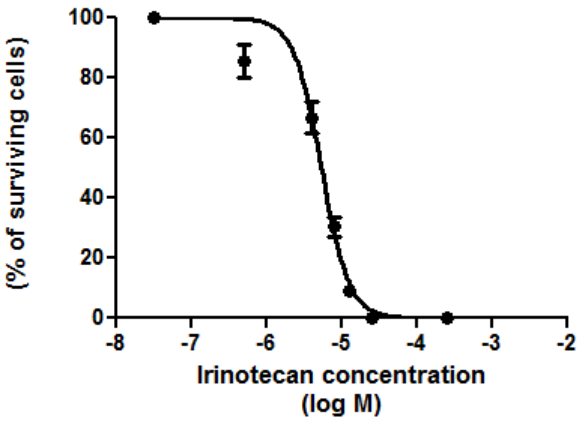

Figure 2

A

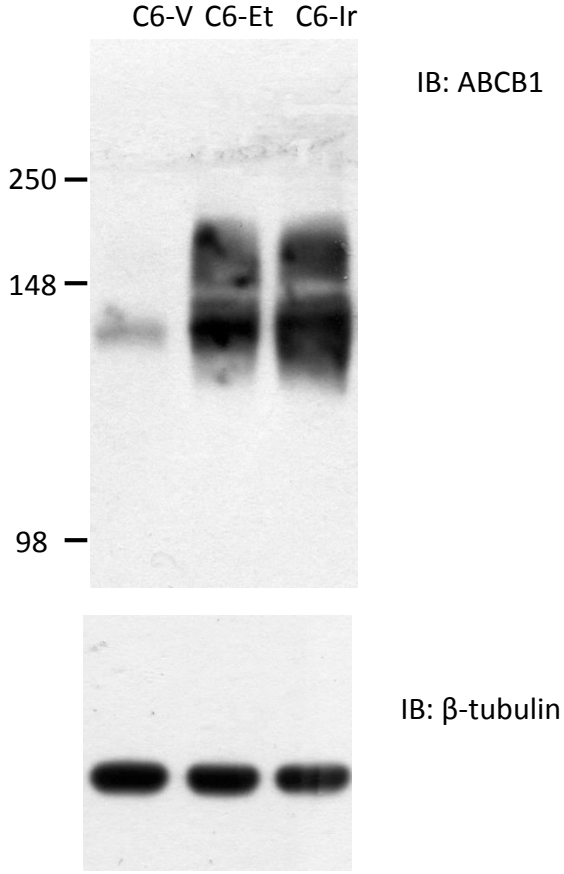
C6-V C6-Et C6-Ir
IB: ABCB1
250
148
98
IB: β-tubulin

B

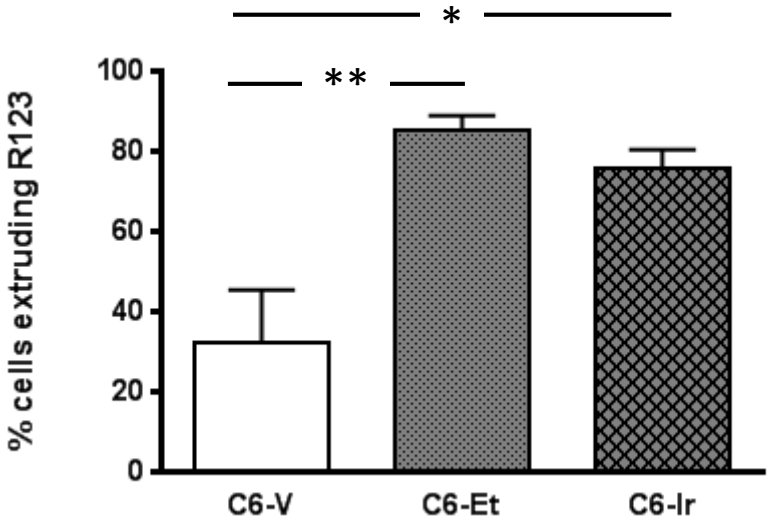
*
**
% cells extruding R123
100
80
60
40
20
0
C6-V
C6-Et
C6-Ir

Figure 3

A

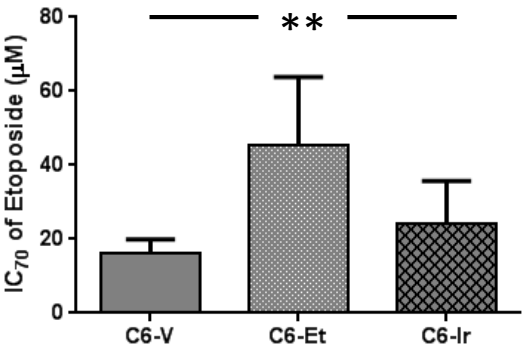
80
60
40
20
0
IC70 of Etoposide (μM)
**
C6-V
C6-Et
C6-Ir

B

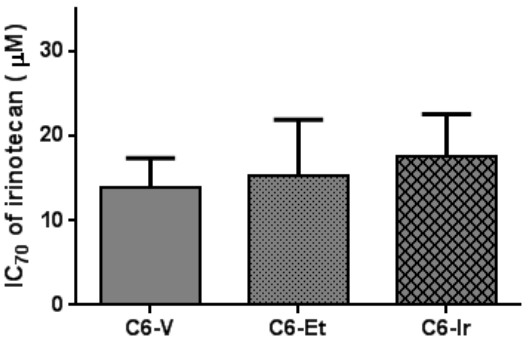
30
20
10
0
IC70 of irinotecan ( μM)
C6-V
C6-Et
C6-Ir

Figure 4

A

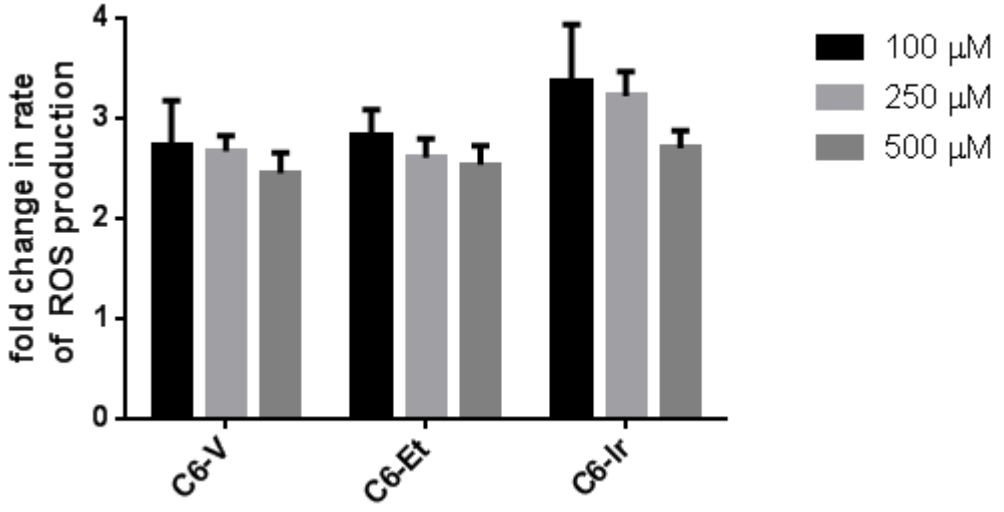
fold change in rate of ROS production
4
3
2
1
0
C6-V
C6-Et
C6-Ir
100 μM
250 μM
500 μM

B

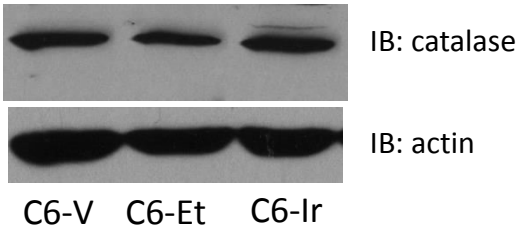
IB: catalase
IB: actin
C6-V
C6-Et
C6-Ir

C

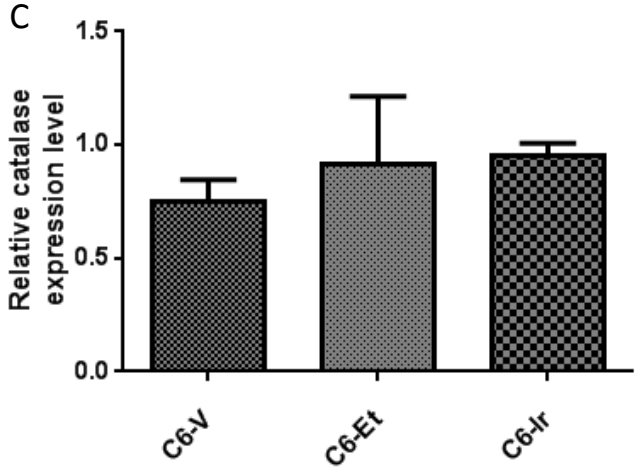
Relative catalase expression level
1.5
1.0
0.5
0.0
C6-V
C6-Et
C6-Ir

Figure 5

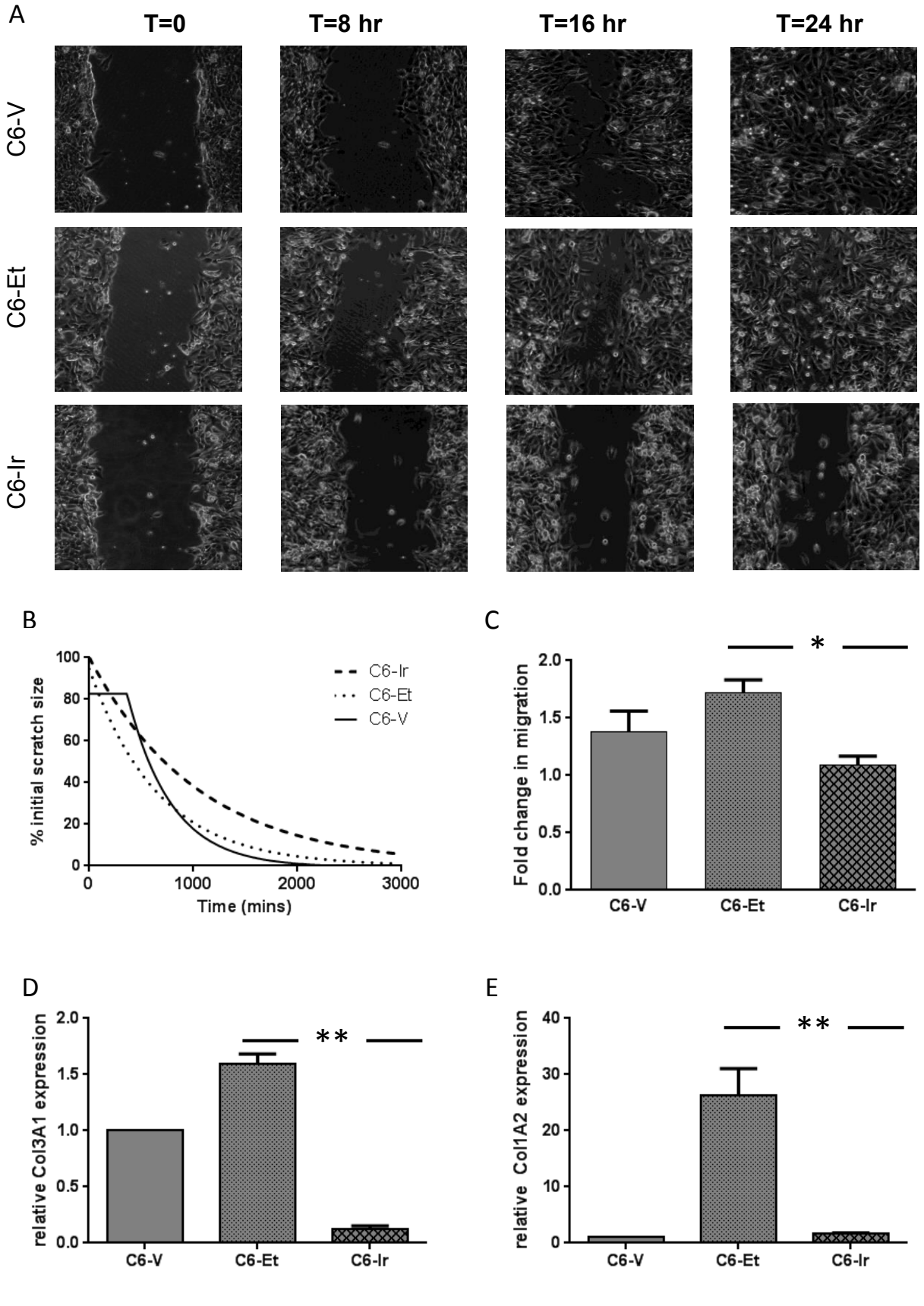
A
T=0
T=8 hr
T=16 hr
T=24 hr
C6-V
C6-Et
C6-Ir
B
% initial scratch size
Time (mins)
C6-Ir
C6-Et
C6-V
C
Fold change in migration
C6-V
C6-Et
C6-Ir
D
relative Col3A1 expression
C6-V
C6-Et
C6-Ir
E
relative Col1A2 expression
C6-V
C6-Et
C6-Ir

**Supplementary Table 1: Primer pairs designed for qRT-PCR**

| Gene | Forward primer | Reverse primer | PCR product size |
|---|---|---|---|
| **COL1A2** | 5’-GCCCGCACATGCCGTGACTT-3’ | 5’-GGGCCTGGATGCAGGTTTCA-3’ | 142 bp |
| **COL3A1** | 5’-TGGTGGACAGATGCTGGTGCTG-3’ | 5’-GGCCCGGCTGGAAAGAAGTCTG-3’ | 150 bp |
| **GAPDH** | 5’-CCCCCTGGCCAAGGTCATCCA-3’ | 5’-CGGCCATCACGCCACAGCTT-3’ | 126 bp |
| **β-Actin** | 5’-ACCGAGGCCCCTCTGAACCC-3’ | 5’-CCAGTGGTACGACCAGAGGCA-3’ | 134 bp |